




Article

Effect of Material Extrusion Method on the Microstructure and Mechanical Properties of Copper Parts

Naiara Aldeiturriaga¹, Itziar Fraile¹ , Erika Dominguez¹, Aitor Zuriarrain², Pedro José Arrazola¹ 
and Daniel Soler^{1,*} 

¹ Faculty of Engineering, Mondragon Unibertsitatea, 20500 Arrasate, Spain; naiara.aldeiturriaga@alumni.mondragon.edu (N.A.); ifraile@mondragon.edu (I.F.); edominguez@mondragon.edu (E.D.); pjarrazola@mondragon.edu (P.J.A.)

² Engineering Department, Campus Goierri–Mondragon Unibertsitatea, 20500 Mondragon, Spain; azuriarrain@mondragon.edu

* Correspondence: dsoler@mondragon.edu

Abstract: In the present study, three extrusion-based Additive Manufacturing (AM) technologies were considered: Fused Filament Fabrication (FFF), Pellet Extrusion Process (PEP) and Atomic Diffusion Additive Manufacturing (ADAM). In order to compare these technologies, the same initial material was employed: a copper filament commercialized by Markforged® (Waltham, MA, USA). The copper filament was employed as received for ADAM and FFF technologies and shredded for PEP technology. Different printing parameters were studied for each technology (except for ADAM, which does not allow it) and the manufactured disc-shaped and tensile test parts were debinded and sintered under the same conditions. Part density, micrography and mechanical properties were analyzed. The density was observed to change with geometry, showing a relative density of around 95% for the tensile test parts through all the technologies but lower relative densities for the disc-shaped parts: around 90% for ADAM, between 85–88% for PEP and between 90–94% for optimized FFF printing parameters. The micrographies present big cavities between infill and contour for ADAM, whereas such cavities were not observed in either PEP or FFF parts. On the other hand, the parts made with PEP showed less and smaller porosity, but they had poor surface finishing, indicating that some printing parameters should be readjusted. Finally, the FFF parts had a better finishing but exhibited a non-uniform pore distribution. Concerning the mechanical properties, all the printed parts show similar properties.

Keywords: copper; pellet; additive manufacturing; metal extrusion; FFF; ADAM



Citation: Aldeiturriaga, N.; Fraile, I.; Dominguez, E.; Zuriarrain, A.; Arrazola, P.J.; Soler, D. Effect of Material Extrusion Method on the Microstructure and Mechanical Properties of Copper Parts. *Metals* **2024**, *14*, 941. <https://doi.org/10.3390/met14080941>

Academic Editors: Abel Dias dos Santos, Abílio M. P. De Jesus and Rui L. Amaral

Received: 24 July 2024

Revised: 11 August 2024

Accepted: 13 August 2024

Published: 17 August 2024



Copyright: © 2024 by the authors. Licensee MDPI, Basel, Switzerland. This article is an open access article distributed under the terms and conditions of the Creative Commons Attribution (CC BY) license (<https://creativecommons.org/licenses/by/4.0/>).

1. Introduction

Additive Manufacturing (AM) has gained great relevance in the manufacturing of complex and spare parts, catching the attention of different industries such as automotive and aviation. Nowadays, AM technologies are applied in the industrial manufacturing of polymeric parts and great effort is being made to achieve this goal for the manufacturing of metallic parts.

There are different AM technologies employed for manufacturing metallic parts and most of them are powder-based, such as Powder Bed Fusion (PBF) [1], Binder Jetting (BJ) [2] and Material Extrusion (ME) [3]. This is the reason why these technologies show many of the problems usually related to Powder Metallurgy. Although a big portion of the issues has already been studied, there are still some challenges to overcome, such as part shrinkage during the sintering process [4], which hinders the implementation of metallic AM technologies in industrial manufacturing.

In the case of PBF and BJ, the powder is applied layer by layer and the part is built inside a chamber full of powder. Consequently, this process presents some handling issues that make them inappropriate for fabrication of prototypes in an office or similar ambient.

However, ME of metals usually employs a polymeric matrix where the metallic powder is trapped in the form of a filament [5] and are considered as desktop printers.

ME includes different type of technologies, but many of them are based on Fused Filament Fabrication (FFF), also known as Fused Deposition Modelling (FDM), consisting in the extrusion of a polymeric filament [6]. Initially, this technology was employed for fabrication of polymeric parts but several years ago Markforged[®] and Desktop Metal brought new solutions for manufacturing of metallic parts based on FFF [7]. Atomic Diffusion Additive Manufacturing (ADAM) was brought to the market by Markforged[®] [8] in 2017, including the debinding and sintering steps necessary to get a metallic part. Desktop Metal developed a similar solution called Bound Metal Deposition (BMD) that differs from the previous one on the shape of the initial materials [9]. In BMD, rods are used, but ADAM and FFF use filaments.

One of the main challenges of this technology for metals is to increase the density of the final part, because it is limited by the load of metallic particles on the filament. Consequently, it is convenient to increase the percentage of metallic particles in the filament, which make the manufacturing process more difficult because the material becomes very brittle [10].

The issue of using highly loaded filaments caused the development of a new technology (based on ME) that uses granulates or pellets as the initial materials, called Fused Granular Fabrication (FGF) [11], Granule-based Material Extrusion (GME) [12] or Pellet Extrusion Process (PEP) [13,14]. PEP brings a significant advantage by streamlining the part manufacturing process through the elimination of filament manufacturing. This approach also enables the recycling or reutilization of defective parts by converting them into nonuniform pellets of new raw material using a shredder, while, for a similar process applied to filament-based systems, the necessity of filament manufacturing would increase the overall cost [15]. Despite the fact that filament-based technologies have historically received more attention [13], there is expected growth in interest in PEP due to already mentioned advantages. However, few studies have already been published regarding the manufacturing of copper parts [16]. Nevertheless, the latest studies have found that PEP parts might show worse mechanical performance than FFF parts [12], but there is still a lot of work to do on this topic.

This work is focused on the comparison of PEP and FFF technologies, as well as on ADAM, taken as a reference because it arrived first to the market as a solution for metallic AM. Therefore, three different systems are used for manufacturing of metallic parts: (i) ADAM: Metal X (commercialized by Markforged[®]), (ii) FFF: adapted Voladora V2 and (iii) PEP: Mini Pro Pellets (both commercialized by Indart3D (Irun, Spain)).

To be able to make a comparison between these three printers and the corresponding manufacturing technologies, it is necessary to employ one material. Due to the properties and limitations presented in the selection of parameters of Metal X, it is not possible to use a material that it is not approved by Markforged[®]. Between the material commercialized by this company, the material selected to perform such a comparison was copper filament.

Copper was chosen due to its excellent electrical and thermal conductivity, which makes it very appropriate to carry out electrical and electronical applications [4]; moreover, due to the current industrial advancements, there is a need for copper parts with complex geometries and optimal mechanical properties, requiring the use of advanced manufacturing technologies. However, common PBF techniques [17] such as Selective Laser Melting (SLM), Direct Metal Laser Sintering (DMLS) and Direct Energy Deposition (DED) are not suitable for copper. Due to copper's high reflectivity, generating high thermal gradients during these processes, achieving high-density and quality parts is very challenging, especially when employing conventional near-infrared laser beams. In the last few years, some studies have been published where visible green and blue wavelength range laser beams are employed as an alternative to near-infrared laser beams in order to process high-reflectivity materials [18]. Consequently, pure copper parts have been difficult to manufacture for different PBF technologies, opening the door for ME, where the properties of copper are not limiting due to its simplicity and the fact that it is done in a non-sintered

state. In addition, this material can be easily oxidized, so the use of powder embedded in a polymeric matrix (pellet or filament) is profitable to avoid powder oxidation during the manufacturing process.

The main goal of this paper is to compare three extrusion-based AM technologies, Fused Filament Fabrication, Pellet Extrusion Process and Atomic Diffusion Additive Manufacturing, which have already been studied [19], considering different printing parameters for each technology, while maintaining the same debinding and sintering processes.

The paper is organized as follows: in the next section, the material and manufacturing systems are described; then, in Section 3, the methods employed for characterizing the manufactured parts are explained and the three systems are compared. Subsequently, obtained results are discussed, leading to the final section where conclusions are drawn.

2. Materials and Manufacturing Systems

As mentioned in the introduction, three printers, Metal X, adapted Voladora V2 and NX Pro Pellets, and their corresponding manufacturing technologies (ADAM, FFF and PEP, respectively) were used. The material employed in this work was copper filament commercialized by Markforged® [20]. The flexibility of this filament (higher than other filaments offered for Metal X) makes it very suitable for FFF. Table 1 shows the chemical composition of the copper powder supplied by the manufacturer.

Table 1. Chemical composition of copper powder (data from Ref. [20]).

Composition	Copper	Oxygen	Iron	Other
Weight %	99.8 min	0.05 max	0.05 max	bal

The NX Pro pellet printer was designed to work with pellets, so it was necessary to process the copper filament in order to convert it to pellets. An automatic homemade shredder was used at Indart3D to cut the filament and fabricate the copper pellets of about 2 mm length that were employed in this work, (see Figure 1).



Figure 1. Pellets obtained after cutting Markforged® copper filament.

Even though the shredder should not apply any change to the material, a ThermoGravimetric Analysis (TGA) of the commercial filament and the prepared pellets was carried out to make sure the behavior of the material, with respect to temperature changes, did not change after the process. The TGA was realized from ambient temperature to 550 °C with a heating rate of 2 °C/min, employing a thermogravimetric analyzer STA 449 F3 Jupiter (NETZSCH, Germany).

Figure 2 shows the thermograms of two samples of copper filament and two samples of copper pellets obtained from the filament. It can be observed that all the thermograms are very similar, showing that the grinding process had no effect on the properties of the polymer remaining in the pellets. The percentage of mass loss presented in Figure 2 is of great relevance, showing that only around 5 wt% was eliminated, which is directly related to the amount of organic material present in the filament. Figure 2 shows the elimination

of the organic material divided into two steps (roughly 200 °C to 300 °C and 300–450 °C), which reveals the presence of two different polymers in the filament/pellets [3].

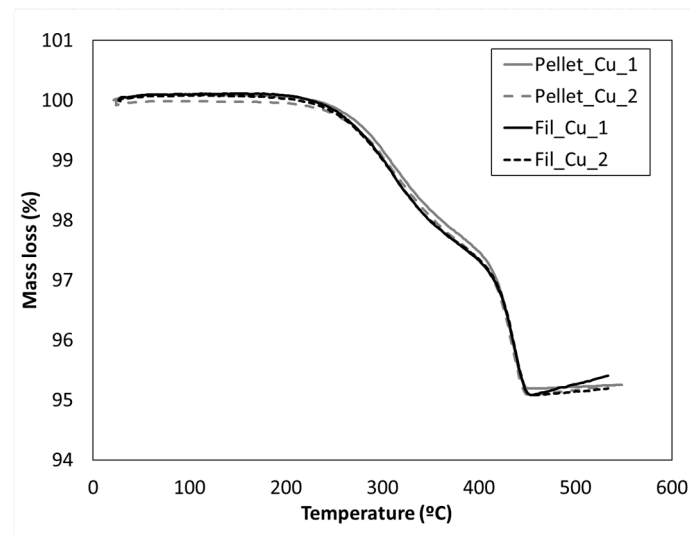


Figure 2. Thermograms of the commercial filament and the pellets obtained after processing the commercial filament.

The powder remaining after TGA was observed in a Nova NanoSEM 450 (FEI, Oregon, USA), a Scanning Electron Microscope (SEM) working with 20 kV of HV, a spot size of 6.0 and a working distance of 5 mm.

As can be seen in Figure 3, the copper powder obtained from the filament and the pellet samples show a similar shape and size distribution. This characterization confirms what was stated by the TGA, that is, there were no changes in the properties of the initial material and, as the processes after shaping the parts were exactly the same for all the specimens, the comparison carried out in this work was focused on the printing/deposition step.

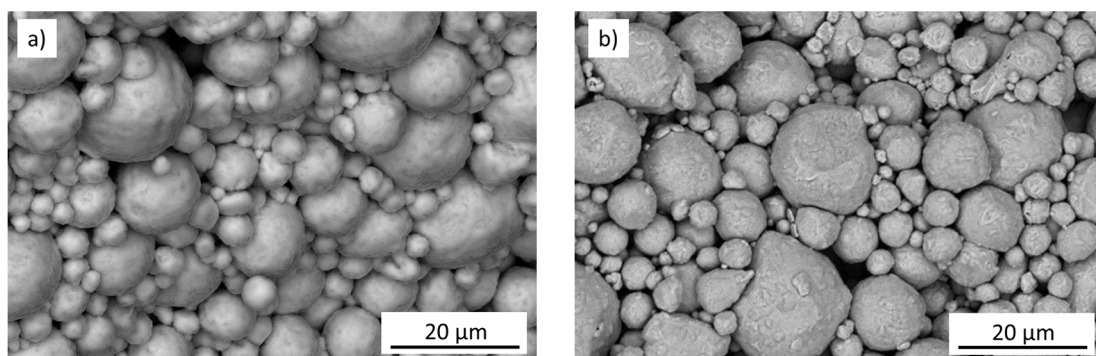


Figure 3. Scanning Electron Microscope (SEM) images of the powder obtained after TGA of (a) the commercial filament and (b) the pellets obtained after processing the commercial filament.

The technologies, printers and printing parameters are described in the following sections.

2.1. Atomic Diffusion Additive Manufacturing (ADAM)

The Metal X system consists of three main steps. The first one is the extrusion step, where the parts are shaped, generating the green part. In this first step, the Metal X system offers the user the opportunity to select the few parameters that were optimized for the selected material by the manufacturer. In this work, the following parameters were employed in order to extrude the desired geometries (see Table 2).

Table 2. Parameters employed of manufacturing MF1 parts using ADAM.

Parameter	MF
Post-sintered Layer Height (mm)	0.129
Fill Pattern	Solid Fill
Wall Layers	2

Once the green part was manufactured, it was taken into the next steps of the Metal X system. Before sintering, it was necessary to apply a debinding step carried out in the Wash-1. This step consists in the elimination of the wax (dissolved in Opteon SF-79 solvent (Chemours, Wilmington, DE, USA)) in order to form porosity that will help in eliminating the rest of the organic components during sintering. It is important to make sure that the part is perfectly dried before introducing it in Sinter-1 for the last sintering step. The Metal X system is highly automatized, which means it facilitates the manufacturing of the part but limits the user's ability to optimize or improve the quality of the part to be fabricated.

As can be seen in Table 2, the specimens generated with this technology were labelled as MF.

2.2. Fused Filament Fabrication (FFF)

Due to the limitations observed in ADAM technology, it is interesting to explore the ability of more opened systems to manufacture metallic parts through ME.

Nowadays, there are many different FFF printers in the market. The Voladora V2 printer was adapted with the help of Indart3D to make it compatible with the manufacturing of a fragile metal powder loaded filament. For that, a direct extruder was mounted in the printer and a holder was located on top of the printer. This modification allowed the manufacturing of copper composite green parts, avoiding issues related to breaking of the filament.

The FFF printer is a fully opened system and allows the adjustment of a huge amount of parameters, allowing the optimization of the printing conditions to the material or geometry employed, thus generating the need to spend some time adjusting the parameters until a good-quality specimen is obtained. Some parameters, see Table 3, were fixed for all the studied conditions.

Table 3. Main parameters employed for manufacturing FFF parts.

Parameter	Value
Bed temperature (°C)	65
Printing speed (mm/min)	125
Infill (%)	100
Outline overlap (%)	15
Layer height (mm)	0.2
Nozzle diameter (mm)	0.4
Extrusion width (mm)	0.48

Only the effect of three parameters were studied in this work, as they were expected to influence on microstructure: extrusion temperature, infill extrusion width and extrusion multiplier.

As can be observed in Table 4, seven sets of parameters were studied in this work, and they were labelled using the notation Fx to denote filament-based material extrusion followed by the condition number.

Table 4. Conditions of different specimens using FFF.

Parameter	F1	F2	F3	F4	F5	F6	F7
Extrusion temperature (°C)	225	225	225	225	225	225	240
Infill extrusion width (%)	100	100	100	100	90	110	100
Extrusion multiplier	1	1.05	1.01	0.95	1	1	1

2.3. Pellet Extrusion Process (PEP)

As the purpose of the study is the comparison between different ME technologies, the parameters employed were selected to be as similar as possible between the different technologies in order to reduce the sources of differences between them.

In Table 5, the parameters that were fixed for the fabrication of the specimens are listed. It is important to note that this printer allowed to control two extrusion temperatures: the slightly lower one on the top of the extruder, whose objective is to ensure a uniform mass of copper and wax for an optimal flow through the extruder, and the bottom extruder temperature, which increases the temperature of the material to an appropriate extrusion temperature.

Table 5. Main parameters employed for manufacturing PEP parts.

Parameter	Value
Upper extrusion temperature (°C)	160
Lower extrusion temperature (°C)	225
Bed temperature (°C)	80
Printing speed (mm)	400
Infill (%)	100
Outline overlap (%)	35
Layer height (mm)	0.2
Nozzle diameter (mm)	0.8
Extrusion width (mm)	0.96

As shown in Table 6, in this case, only two parameters were labeled in order to see their effect in the final part: as in the case of FFF, they were the Extrusion Multiplier and Flow, which is the rotation velocity of the extruder. Therefore, only three parameter sets, labeled as Px, show that the technology employed was pellet-based ME and the corresponding numbers were considered.

Table 6. Conditions of different specimens using PEP.

Parameter	P1	P2	P3
Flow (rpm)	325	325	275
Extrusion multiplier	1	0.8	0.8

3. Methods

Two types of specimens were manufactured, disc-shaped samples and tensile specimens: (i) disc-shaped samples, two for each printing condition, for density measurements and microstructure analysis, and to relate the presence of porosity and its shape to the mechanical properties of the parts. The geometry of these specimens was about 4 mm in height and 12 mm in diameter after the sintering process; however, not all specimens had the same final dimensions. PEP specimens, being somewhat flatter, were approximately 2.8 mm in height and 11.5 mm in diameter, and the FFF specimens, being somewhat larger,

had a diameter of approximately 13 mm; (ii) tensile specimens, which were fabricated at each of the following conditions: P1, P2, F1 and F7. Concretely, there were three specimens for each condition, and six extra specimens of MF. All specimens were manufactured with a solid infill pattern.

3.1. Density Measurements

The Standard ASTM B962 [21] was followed for density measurements. Part density (ρ_p) and relative density (RD) values were calculated as described in a previous work [3]. Disc-shaped samples and tensile test specimens were used for density measurements. For each sample there were performed at least three measurements.

3.2. Porosity Analysis

As two samples were manufactured for each condition, the longitudinal section and the cross-section of the geometry could be studied. In Figure 4, the sample prepared for microstructure analysis of MF can be observed. Thus, the contour-infill interface and layer-layer interface can be studied and compared.

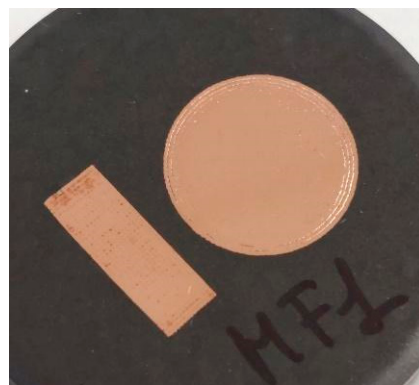


Figure 4. Image of the MF sample prepared for microstructure analysis, showing two different parts manufactured at the same conditions, positioned to study the longitudinal and cross-section of the part.

The porosity of the samples was observed in a FEI Nova NanoSEM 450, a Scanning Electron Microscope (SEM) working with 20 kV of HV, a spot size of 6.0 and a working distance of 5 mm.

3.3. Tensile Tests

The tensile specimens were fabricated following the dimensions defined by Abe et al. [22] and illustrated in Figure 5.

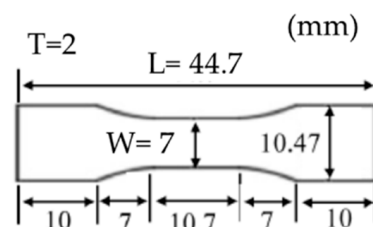


Figure 5. Tensile specimen dimensions (L = length; W = width; T = thickness) (data from Ref. [22]).

The tensile tests were carried out using the universal machine TN-MD-200 (HOYTOM, Bizkaia, Spain). All the tensile tests were carried out with a strain rate of 0.2 mm/min in the elastic zone and 2 mm/min in the plastic zone.

4. Results and Discussion

First, as can be seen in Figure 6, the external appearance of the specimens varied significantly depending on the technology employed. It is important to highlight that the application of FFF and PEP for printing metallic parts is still under development, and as previously mentioned, there are numerous printing parameters that can be adjusted to achieve improved outcomes.



Figure 6. Some examples of green parts corresponding to the three processes, PEP, FFF and ADAM. (a) P2, (b) F1 and (c) MF.

4.1. Density Measurements

The results regarding density measurements of disc-shaped samples are listed in Table 7, where reported values correspond to the mean of performed measurements of different samples at the same printing condition set.

Table 7. Values of density and relative density of disc-shaped parts manufactured at different conditions.

Conditions.	Density (g/cm ³)		Relative Density	
	Mean	Deviation	Mean	Deviation
MF	8.012	0.003	0.894	0.003
P1	7.583	0.005	0.846	0.012
P2	7.851	0.005	0.876	0.009
P3	7.848	0.001	0.876	0.002
F1	8.213	0.083	0.917	0.009
F2	8.176	0.073	0.913	0.008
F3	8.153	0.071	0.910	0.008
F4	8.079	0.100	0.902	0.011
F5	8.162	0.159	0.911	0.018
F6	8.250	0.124	0.921	0.014
F7	8.411	0.211	0.939	0.024

Samples fabricated through PEP show a density between 7.5 and 7.9 g/cm³ (RD of 85–88%), which is lower than the density obtained through ADAM. (Some specimens had an RD lower than MF, as could be understood by considering the standard deviations.) However, the density of samples manufactured through FFF is, in nearly all the cases, higher than the reference (MF). In particular, the highest density obtained is under the F7 condition with a density of around 8.4 g/cm³ (RD of roughly 94%), a density increase of 5%, with respect to the MF results.

As mentioned in Section 3.3, tensile tests were performed with specimens manufactured with different techniques. Figure 7 shows the three samples before the sintering process that were used to perform such tests. It is remarkable that, while the surface finishing of MF samples was better than those manufactured with PEP and FFF, differences were not as significant as in the case of the disc-shaped parts shown in Figure 6.



Figure 7. Some examples of green parts corresponding to the three processes: (a) P2, (b) F1 and (c) MF.

The results obtained through tensile test specimens (Table 8) reveals very different results. Surprisingly, the differences between samples observed in Table 7 are not observed in this case. All the density measurements presented in Table 8 are very similar and are located around 8.5 g/cm^3 (RD of roughly 95%), independently of the conditions employed for sample fabrication, suggesting the effect of sample geometry on density.

Table 8. Values of density and relative density of the specimens for tensile test manufactured at different conditions.

Conditions	Density (g/cm^3)		Relative Density	
	Mean	Deviation	Mean	Deviation
MF	8.490	0.064	0.948	0.007
P2	8.493	0.017	0.948	0.002
F1	8.494	0.121	0.948	0.014
F7	8.494	0.058	0.948	0.006

The values for density obtained in this section are comparable with the measurements reported in previous works. Ren et al. [23] reported a density of $8.15 \frac{\text{g}}{\text{cm}^3}$ for copper parts manufactured through ME, which is lower than the values obtained in this study for tensile test specimens (see Table 8) manufactured through any of the selected technologies. However, the values for relative density obtained in this work are not as high as the ones obtained through other AM technologies such as Electron Beam Melting (EBM), reported [24] to be $8.84 \frac{\text{g}}{\text{cm}^3}$.

As copper parts manufactured through ADAM technology are used as a reference, it is important to note that the relative density measured in this work for all the geometries was around 90–95%, while the relative density reported by Markforged® in the official datasheet is 98% [20]. In general, the relative densities achieved with PEP and FFF are quite similar to the ones reported by Hwang et al. [25] (92.1–95.5%) where FFF technology was employed. However, Singh et al. [16] reported a relative density of 91% for copper parts manufactured through PEP, much lower than the results presented in Table 8 for the same technology. Thus, showing that material composition, printing parameters and debinding and sintering steps are of great relevance for achieving a high density. Therefore, it is clear that the optimization of those steps could lead to better final part properties, independently of the employed technology (PEP, FFF or ADAM).

4.2. Porosity Analysis

This section is focused on the microstructure observed for each condition, but it is important to take into account the close relation between density measurements and the amount of porosity observed in the microstructure. As stated in Section 3.2, only disc-shaped parts were considered for this analysis.

First, we analyze the reference sample (MF). Its microstructure is presented in Figure 8. Taking into account that the density was about 89%, some porosity was expected. On the one hand, concerning the longitudinal section, as shown in Figure 8a, the contour

rasters and its contact area with the infill was not well-linked and formed big cavities. However, the porosity in the infill zone, as shown in Figure 8b, is not really significant. On the other hand, the microstructure of the cross-section of the sample (Figure 8c,d) shows the formation of small cavities in the junction between layers and rasters. These defects appear all over the cross-section, being more notorious in the contour because, as seen in the longitudinal section, the junction between contour rasters is worse than in the infill. Apart from this bigger porosity, there are also micropores distributed all over the sample. This porosity distribution is similar to the ones studied previously in other works [3].

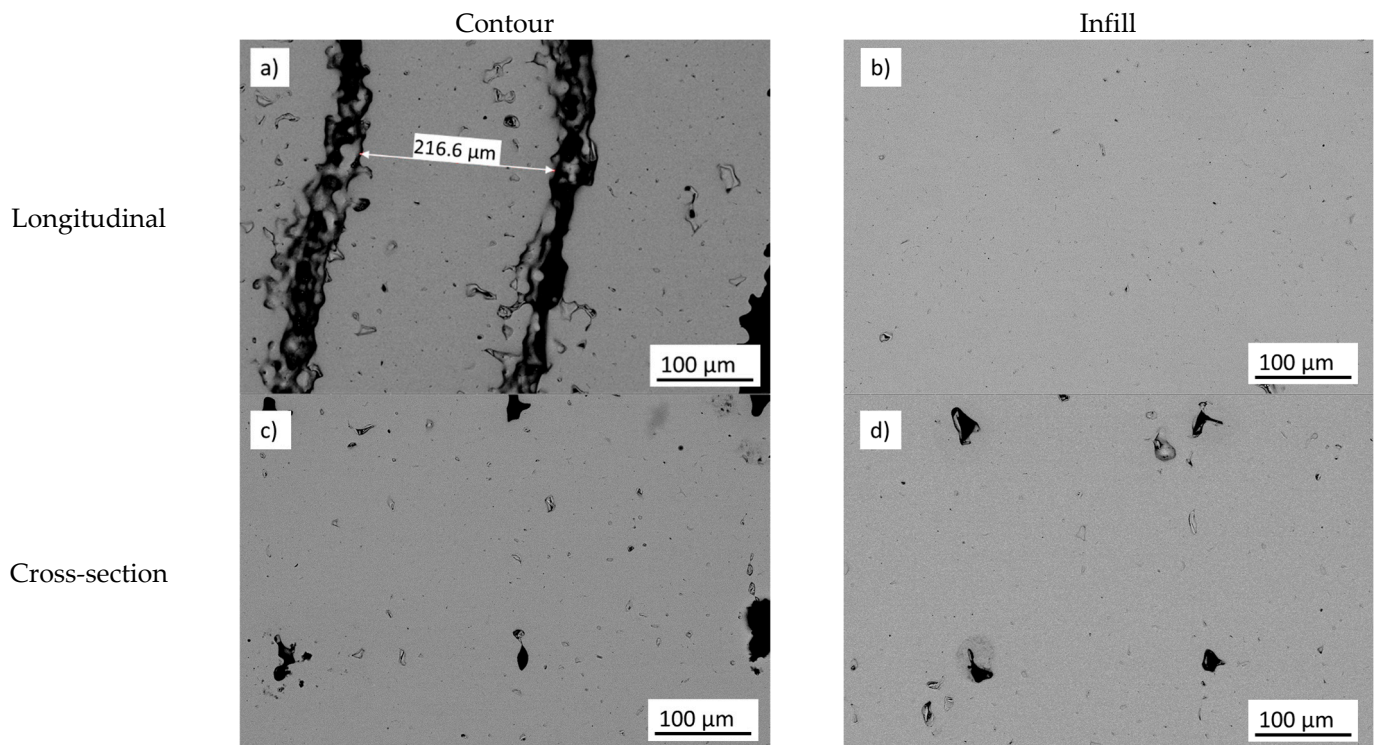


Figure 8. SEM images of longitudinal sections (a,b) and cross-sections (c,d) of the MF parts.

Figure 9 shows the longitudinal section and cross-section of parts manufactured by PEP, with all pictures taken in the infill/contour zone. A first analysis reveals that the porosity that is observed in the longitudinal section of sample P1 is remarkable, especially at the contour in the righthand side of the image, but no cavities were observed between the contour and infill (see Figure 9a), while the cross-section of P1 (Figure 9b) shows less porosity and no cavities between the layers or rasters. The low value of relative density (see Table 7) is therefore related to the bad surface finishing that can be observed in Figure 6a, where this sample was presented due to the high amount of material extruded in its fabrication and not to an internal porosity.

In P2, as the extrusion multiplier was decreased, the amount of extruded material was reduced. The obtained microstructure is shown in Figure 9c,d, where less porosity is observed and it has rounded shape, suggesting it has a different origin. A closer look on the longitudinal section does not give additional information, but the porosity in the cross section was not randomly distributed. The porosity in Figure 9d appears to be forming horizontal lines that can be related to the junction between different layers, suggesting there is not good adhesion between layers. Nevertheless, the adhesion was better than in the MF sample.

The microstructure of sample P3 (shown in Figure 9e,f) is very similar to the previous one, as their values for density and relative density suggest (see Table 7). There is no presence of big cavities between the contour and the infill and the longitudinal section

presents a homogeneous distribution of porosity (Figure 9e). As in the previous case, the cross-section shows porosity orientation related to the junction between layers.

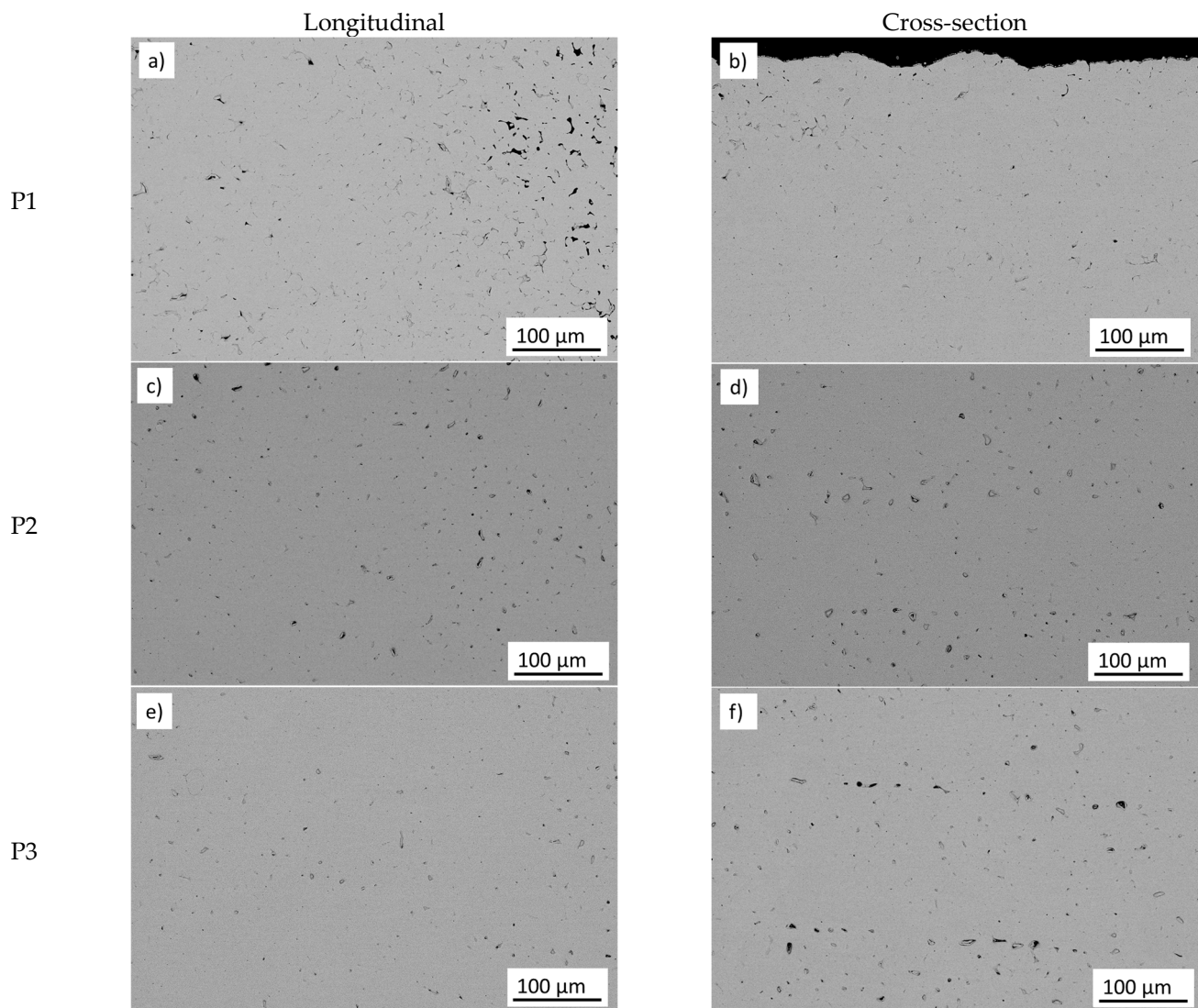


Figure 9. SEM images of the longitudinal sections (a,c,e) and cross-sections (b,d,f) of the parts manufactured at P1, P2 and P3 conditions.

In the case of the samples fabricated through FFF, the microstructure of the parts manufactured at conditions F1 to F4 are presented in Figure 10, and F5 to F7 are shown in Figure 11. This arrangement is meant to facilitate comparison due to the parameters varied in each condition. So, Figure 10 allows us to study the effect of the extrusion multiplier, and Figure 11 collects the variations in extrusion temperature (F7) and infill extrusion width (F5 and F6) to be compared with F1.

As shown in Table 7, parts manufactured at F1 condition had a higher density than the reference (MF). This is mainly related to the absence of cavities between contour and infill rasters (see Figure 10a,b); however, F1 shows more small pores inside the rasters than MF, which could be due to the formation of gas/air bubbles during the deposition process or inhomogeneities in the deposition pattern. It is important to remark that the cross-section of F1 shows homogeneous porosity distribution indicating that the adhesion between the layers is good enough.

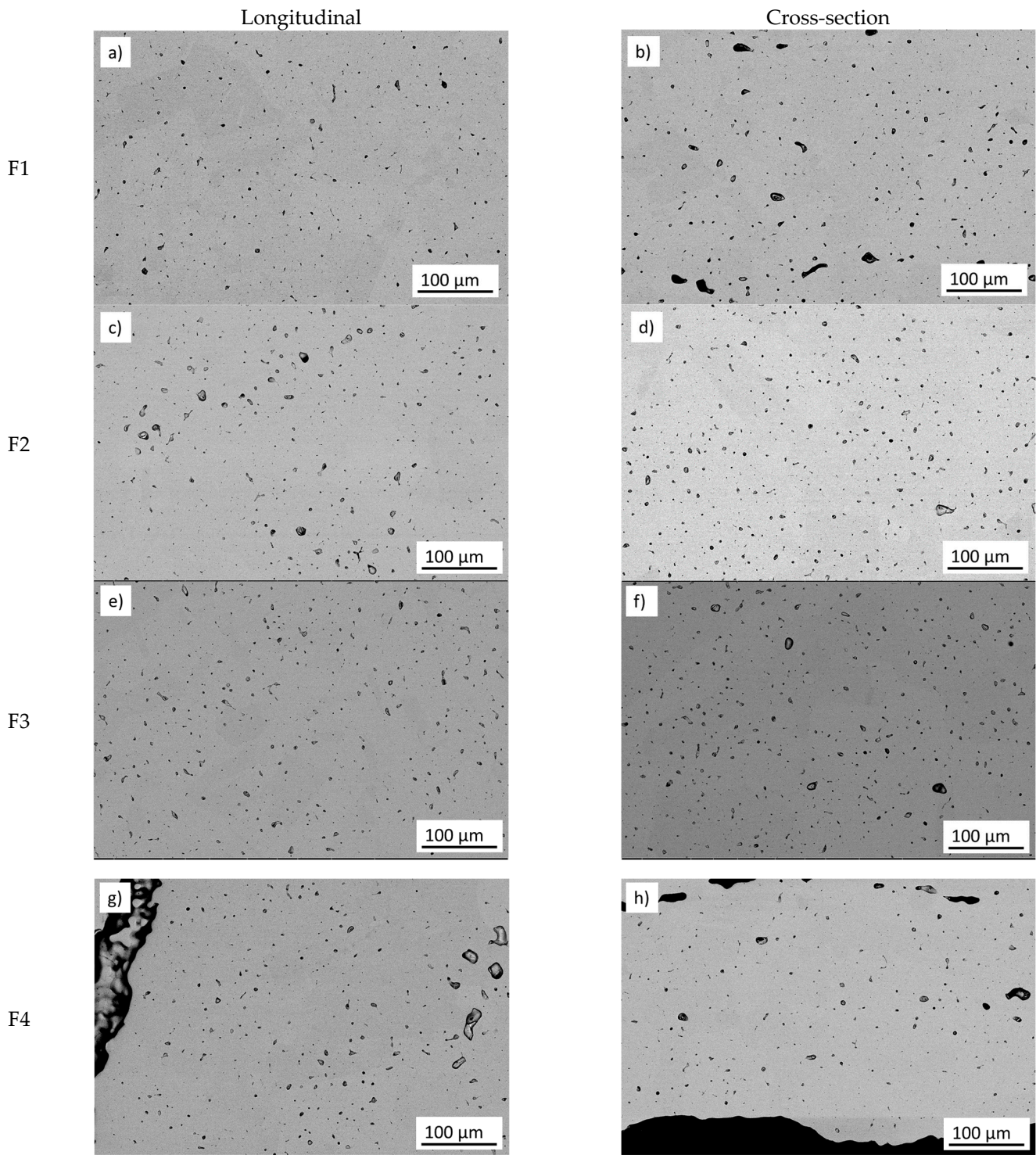


Figure 10. SEM images of longitudinal sections (a,c,e,g) and cross-sections (b,d,f,h) of the parts manufactured at F1 to F4 conditions.

Increasing the value for the extrusion multiplier does not seem to change the density of the part (see Table 7). This is confirmed through the analysis of microstructures corresponding to F2 and F3 (see Figure 10c–f) where the porosity observed is similar to the one for F1 (Figure 10a,b) and does not show a relation to layer or raster direction.

Nevertheless, when the extrusion multiplier was less than 1, the density of the part was decreased as it increased the porosity (see Figure 10g,h). In this case, a lack of stickiness between rasters and layers can be observed.

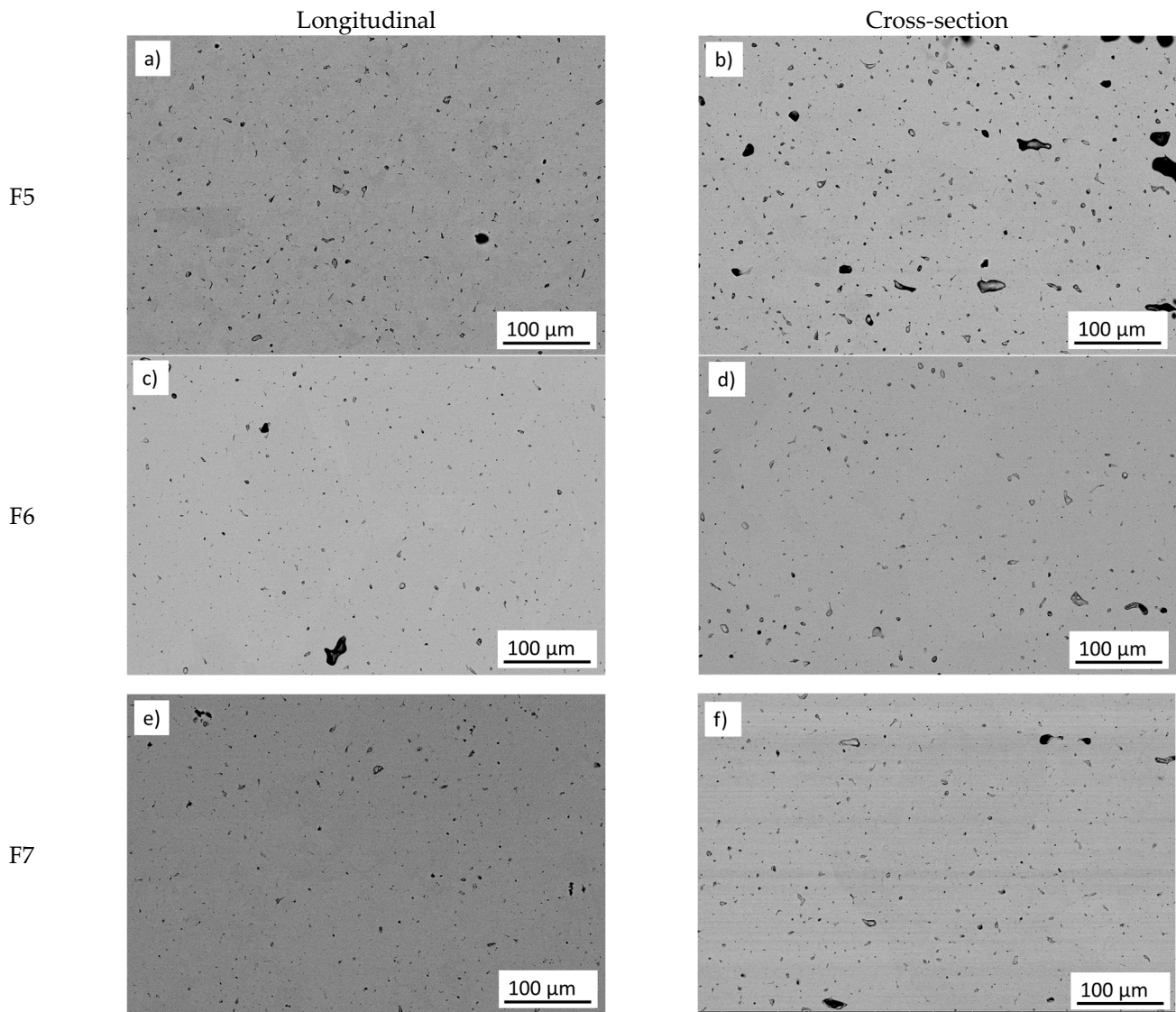


Figure 11. SEM images of longitudinal sections (a,c,e) and cross-sections (b,d,f) of the parts manufactured at F5 F6 and F7 conditions.

Moreover, in Figure 10h, the alignment of irregular porous can be observed corresponding to the junction between the second and third layers. In addition, Figure 10g shows the presence of a big cavity formed in the limits between the contour and infill rasters.

The effect of infill extrusion width can be observed in Figure 11a–d and can be compared with Figure 10a,b. The last one corresponds to an infill extrusion width of 100%, while Figure 11a,b correspond to a value of 90% and Figure 11c,d, belong to a value of 110%. Apparently, the reduction of this parameter leads to the formation of bigger holes or cavities between different layers (as seen in the cross-sections), giving worse adhesion between layers, with the corresponding decrease in density (see Table 7).

Finally, the effect of extrusion temperature can be analyzed through the inspection of Figure 11e,f corresponding to a temperature of 240 °C, and Figure 10a,b, corresponding to a temperature of 225 °C. Figure 11e shows a similar porous distribution compared with Figure 10a, but it seems to present less porosity. Having a look at the porosity of both cross-sections (Figures 10b and 11f), the porosity presented on the part manufactured at 225 °C is higher in size and number than the one presented on the part manufactured at 240 °C.

4.3. Mechanical Properties

Figure 12 shows a stress-strain curve for each printing condition.

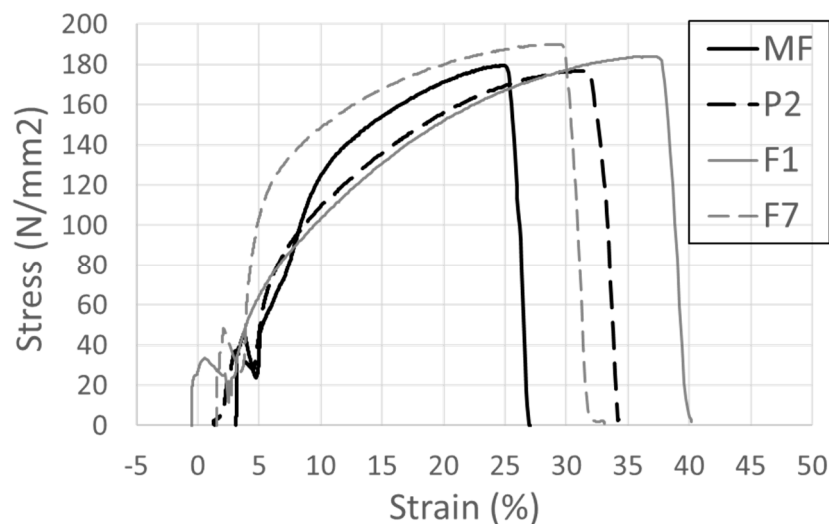


Figure 12. Stress-strain curves of tensile specimens. Only one curve for each printing condition is shown.

After the analysis of these curves and the corresponding to other specimens, the obtained results of tensile tests are given in Table 9. The given values are the arithmetic means of performed tests and the uncertainty is given by the corresponding standard deviation.

Table 9. Yield strength, tensile strength and maximum elongation of tested specimens and some literature values.

	Yield Strength (MPa)	Tensile Strength (MPa)	Maximum Elongation (%)
MF	38.9 ± 1.2	181 ± 8	37.5 ± 0.7
P2	38.5 ± 5.7	178.4 ± 1.5	33.0 ± 1.4
F1	38.4 ± 4.4	185 ± 3	38.2 ± 3.1
F7	45.2 ± 7.0	177 ± 20	26.5 ± 8.5
Markforged datasheet [20]	26	193	45

Experimental measurements can be compared (see Table 9) with the mechanical properties reported in Markforged's material datasheet for copper [20]. On the one hand, the maximum elongation achieved for copper parts manufactured through ADAM technology are lower than the reported one, but very similar to the parts fabricated using FFF at F1 conditions. On the other hand, the parts manufactured at P2 conditions (PEP) show lower maximum elongation; however, this property is expected to be higher through the optimization of the printing parameters. The relevance in printing parameters is presented in the results for F1 and F7, whose difference is based on the change of Extrusion Temperature.

Regarding the Tensile Strength (see Table 9), it can be concluded that the experimental measurements are very similar for all the technologies at tested conditions, but are lower than the theoretical one. However, focusing on yield strength, all the experimental measurements are higher than the theoretical value. In this case, it is especially remarkable the value obtained at F7 condition, that is higher than the others (which are pretty similar). These results come along with the yield strength reported by Ren et al. [23] for copper parts manufactured through Material Extrusion. Ren et al. obtained a yield strength of 51 MPa, very close to the value obtained in this study for the F7 condition.

Concerning these mechanical properties, except maximum elongation, which can be seen in Figure 13, the F7 specimen showed the smallest value, and no substantial difference

was detected between different specimens, as considering reported uncertainties, the same values could be associated with all parts. This uniformity is consistent with density results shown in Table 8. Moreover, it confirms that poor surface finishing obtained with PEP is not related to infill defects, as shown by micrography pictures, because it does not significantly affect its mechanical behavior.

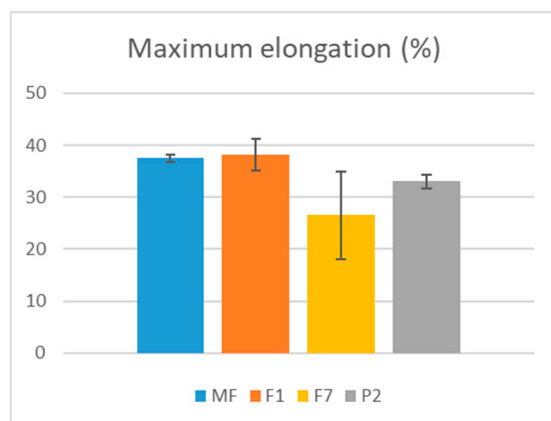


Figure 13. Comparison of maximum between different specimens.

5. Conclusions and Further Work

There are some conclusions that could be depicted from the previous sections:

- According to that discussed in Section 4, the capacity to determine some parameters of the printing strategy allows to overcome the problem of the lack of addition between layers that is observed with the close printer Metal X of Markforged®.
- Density measurements seem to indicate that not only the printing conditions determine the density of the part, but that it could also be conditioned by the final geometry of the part, suggesting that printing strategy may be conditioned to the final geometry of the part.
- Parts manufactured by PEP showed lower pore density and smaller pores than those based on filament extrusion, confirming that it could be a very promising technology.
- No relevant differences in mechanical behavior were found between parts built using different ME technologies. Especially regarding the advantages of PEP technology detailed in the introduction, this conclusion is of great relevance, showing that the mechanical behaviour and density of PEP manufactured copper parts is similar to copper parts manufactured through FFF and ADAM.

To improve the current results for PEP in future works, we aim to expand the parameters to be modified for printing optimization. In fact, we have already printed disc-shaped and tensile parts by modifying the nozzle diameter to 0.4 mm, resulting in better surface finishing. Additionally, the density of the disc-shaped parts was improved, but the tensile parts showed lower density and poorer mechanical properties. This reinforces the idea that the final geometry should dictate the printing conditions.

Author Contributions: Conceptualization, I.F., A.Z. and D.S.; methodology, I.F.; validation, I.F., P.J.A. and D.S.; formal analysis, I.F. and D.S.; investigation, N.A., I.F., E.D. and D.S.; resources, A.Z.; data curation, N.A., I.F. and E.D.; writing—original draft preparation, I.F. and D.S.; writing—review and editing, D.S.; visualization, N.A.; supervision, A.Z. and P.J.A.; project administration, P.J.A.; funding acquisition, P.J.A. All authors have read and agreed to the published version of the manuscript.

Funding: The authors would like to thank the Basque Government for the financial support to the projects Ekoprop II (KK-2024/00102) and COPEFI (BDI-2023-00029).

Data Availability Statement: The original contributions presented in the study are included in the article, further inquiries can be directed to the corresponding author.

Acknowledgments: The authors would like to thank the technical support given by Indart3D.

Conflicts of Interest: The authors declare no conflicts of interest.

References

1. Strondl, A.; Lyckfeldt, O.; Brodin, H.; Ackelid, U. Characterization and Control of Powder Properties for Additive Manufacturing. *JOM* **2015**, *67*, 549–554. [CrossRef]
2. Mao, Y.; Cai, C.; Zhang, J.; Heng, Y.; Feng, K.; Cai, D.; Wei, Q. Effect of Sintering Temperature on Binder Jetting Additively Manufactured Stainless Steel 316L: Densification, Microstructure Evolution and Mechanical Properties. *J. Mater. Res. Technol.* **2023**, *22*, 2720–2735. [CrossRef]
3. Rodriguez, J.; Zuriarrain, A.; Madariaga, A.; Arrazola, P.J.; Dominguez, E.; Fraile, I.; Soler, D. Mechanical Properties and Fatigue Performance of 17-4 PH Stainless Steel Manufactured by Atomic Diffusion Additive Manufacturing Technology. *J. Manuf. Mater. Process.* **2023**, *7*, 172. [CrossRef]
4. Huber, D.; Vogel, L.; Fischer, A. The Effects of Sintering Temperature and Hold Time on Densification, Mechanical Properties and Microstructural Characteristics of Binder Jet 3D Printed 17-4 PH Stainless Steel. *Addit. Manuf.* **2021**, *46*, 102114. [CrossRef]
5. Henry, T.C.; Morales, M.A.; Cole, D.P.; Shumeyko, C.M.; Riddick, J.C. Mechanical Behavior of 17-4 PH Stainless Steel Processed by Atomic Diffusion Additive Manufacturing. *Int. J. Adv. Manuf. Technol.* **2021**, *114*, 2103–2114. [CrossRef]
6. Di Angelo, L.; Di Stefano, P.; Marzola, A. Surface Quality Prediction in FDM Additive Manufacturing. *Int. J. Adv. Manuf. Technol.* **2017**, *93*, 3655–3662. [CrossRef]
7. Bankapalli, N.K.; Gupta, V.; Saxena, P.; Bajpai, A.; Lahoda, C.; Polte, J. Filament Fabrication and Subsequent Additive Manufacturing, Debinding, and Sintering for Extrusion-Based Metal Additive Manufacturing and Their Applications: A Review. *Compos. B Eng.* **2023**, *264*, 110915. [CrossRef]
8. Campbell, I.; Wohlers, T. Markforged: Taking a Different Approach to Metal Additive Manufacturing. 2017. Available online: https://repository.lboro.ac.uk/articles/journal_contribution/Markforged_Taking_a_different_approach_to_metal_Additive_Manufacturing/9346493?file=16955546 (accessed on 16 August 2024).
9. Metal, D. BMD Design Guide. 1–15. Available online: <https://www.desktopmetal.com/resources/bmd-design-guide> (accessed on 16 August 2024).
10. Dey, A.; Eagle, I.N.R.; Yodo, N. A Review on Filament Materials for Fused Filament Fabrication. *J. Manuf. Mater. Process.* **2021**, *5*, 69. [CrossRef]
11. Kalle, J.; Joni, K.; Alexander, S.; Juhani, O. Potential and Challenges of Fused Granular Fabrication in Patternmaking. *Int. J. Met.* **2023**, *17*, 2469–2476. [CrossRef]
12. Liu, H.; Gong, K.; Portela, A.; Cao, Z.; Dunbar, R.; Chen, Y. Granule-Based Material Extrusion Is Comparable to Filament-Based Material Extrusion in Terms of Mechanical Performances of Printed PLA Parts: A Comprehensive Investigation. *Addit. Manuf.* **2023**, *75*, 103744. [CrossRef]
13. Gupta, A.K.; Taufik, M. Effect of Process Variables on Performances Measured in Filament and Pellet Based Extrusion Process. *Mater. Today Proc.* **2021**, *47*, 5177–5184. [CrossRef]
14. Pricci, A.; de Tullio, M.D.; Percoco, G. Analytical and Numerical Models of Thermoplastics: A Review Aimed to Pellet Extrusion-Based Additive Manufacturing. *Polymers* **2021**, *13*, 3160. [CrossRef] [PubMed]
15. Bocchi, S.; Urso, G.D.; Giardini, C.; Carminati, M.; Borriello, C.; Tammara, L.; Galvagno, S. Reuse of Green Parts for Metal Material Extrusion: A Recycling Approach for Improved Sustainability. *J. Clean. Prod.* **2024**, *434*, 140165. [CrossRef]
16. Singh, G.; Missiaen, J.M.; Bouvard, D.; Chaix, J.M. Copper Extrusion 3D Printing Using Metal Injection Moulding Feedstock: Analysis of Process Parameters for Green Density and Surface Roughness Optimization. *Addit. Manuf.* **2021**, *38*, 101778. [CrossRef]
17. Rocchetti Campagnoli, M.; Galati, M.; Saboori, A. On the Processability of Copper Components via Powder-Based Additive Manufacturing Processes: Potentials, Challenges and Feasible Solutions. *J. Manuf. Process.* **2021**, *72*, 320–337. [CrossRef]
18. Grub, P.; Hofele, M.; Schanz, J.; Kolb, D.; Riegel, H. Laser Polishing of Additive Manufactured L-PBF Copper Parts with Visible Laser Wavelength of 515 Nm—Challenges Due to High Surface Roughness. *Procedia CIRP* **2022**, *111*, 684–688. [CrossRef]
19. Basha, S.M.; Venkaiah, N.; Sankar, M.R. Development and Performance Evaluation of Galactomannan Polymer Based Abrasive Medium to Finish Atomic Diffusion Additively Manufactured Pure Copper Using Abrasive Flow Finishing. *Addit. Manuf.* **2023**, *61*, 103290. [CrossRef]
20. Markforged Material Datasheet: Copper. 2023. Available online: https://markforged.com/materials/metals/copper?__geom=%E2%9C%AA (accessed on 16 August 2024).
21. ASTM B962; Standard Test Methods for Density of Compacted or Sintered Powder Metallurgy (PM) Products Using Archimedes' Principle. Available online: https://global.ihs.com/doc_detail.cfm?document_name=ASTM%20B962&item_s_key=00517308 (accessed on 2 March 2023).
22. Abe, Y.; Kurose, T.; Santos, M.V.A.; Kanaya, Y.; Ishigami, A.; Tanaka, S.; Ito, H. Effect of Layer Directions on Internal Structures and Tensile Properties of 17-4PH Stainless Steel Parts Fabricated by Fused Deposition of Metals. *Materials* **2021**, *14*, 243. [CrossRef] [PubMed]
23. Ren, L.; Zhou, X.; Song, Z.; Zhao, C.; Liu, Q.; Xue, J.; Li, X. Process Parameter Optimization of Extrusion-Based 3D Metal Printing Utilizing PW-LDPE-SA Binder System. *Materials* **2017**, *10*, 305. [CrossRef] [PubMed]

24. Frigola, P.; Harrysson, O.; Horn, T.; West, H.; Aman, R.; Rigsbee, J.; Ramirez, D.; Medina, F.; Wicker, R.; Rodriguez, E. Fabricating Copper Components. *Adv. Mater. Process.* **2014**, *20*. [[CrossRef](#)]
25. Hwang, J.Y.; Jung, H.Y. Electrical Conductivity upon Sintering of Pure Cu Produced by Material Extrusion Additive Manufacturing: Effects of Pore, Grain Size, and Impurity. *J. Manuf. Process.* **2024**, *118*, 63–75. [[CrossRef](#)]

Disclaimer/Publisher’s Note: The statements, opinions and data contained in all publications are solely those of the individual author(s) and contributor(s) and not of MDPI and/or the editor(s). MDPI and/or the editor(s) disclaim responsibility for any injury to people or property resulting from any ideas, methods, instructions or products referred to in the content.